

RESEARCH ARTICLE

Dual biomarkers long non-coding RNA GAS5 and microRNA-34a co-expression signature in common solid tumors

Eman A. Toraih^{1,2*}, Saleh Ali Alghamdi³, Aya El-Wazir^{1,2}, Marwa M. Hosny⁴, Mohammad H. Hussein⁵, Moataz S. Khashana⁶, Manal S. Fawzy^{6,7*}

1 Genetics Unit, Department of Histology and Cell Biology, Faculty of Medicine, Suez Canal University, Ismailia, Egypt, **2** Center of Excellence of Molecular and Cellular Medicine, Suez Canal University, Ismailia, Egypt, **3** Medical Genetics, Clinical Laboratory Department, College of Applied Medical Sciences, Taif University, Taif, Saudi Arabia, **4** Department of Medical Biochemistry and Molecular Biology, Faculty of Medicine, Suez Canal University, Ismailia, Egypt, **5** Ministry of Health and Population, Cairo, Egypt, **6** Faculty of Medicine, Suez Canal University, Ismailia, Egypt, **7** Department of Biochemistry, Faculty of Medicine, Northern Border University, Arar, Saudi Arabia

* manal2_khashana@gmail.com (MSF); emantoraih@gmail.com (EAT)



OPEN ACCESS

Citation: Toraih EA, Alghamdi SA, El-Wazir A, Hosny MM, Hussein MH, Khashana MS, et al. (2018) Dual biomarkers long non-coding RNA GAS5 and microRNA-34a co-expression signature in common solid tumors. PLoS ONE 13(10): e0198231. <https://doi.org/10.1371/journal.pone.0198231>

Editor: Aamir Ahmad, University of South Alabama Mitchell Cancer Institute, UNITED STATES

Received: May 14, 2018

Accepted: September 16, 2018

Published: October 5, 2018

Copyright: © 2018 Toraih et al. This is an open access article distributed under the terms of the [Creative Commons Attribution License](https://creativecommons.org/licenses/by/4.0/), which permits unrestricted use, distribution, and reproduction in any medium, provided the original author and source are credited.

Data Availability Statement: All relevant data are within the paper and its Supporting Information files.

Funding: The author(s) received no specific funding for this work.

Competing interests: The authors have declared that no competing interests exist.

Abstract

Accumulating evidence indicates that non-coding RNAs including microRNAs (miRs) and long non-coding RNAs (lncRNAs) are aberrantly expressed in cancer, providing promising biomarkers for diagnosis, prognosis and/or therapeutic targets. We aimed in the current work to quantify the expression profile of miR-34a and one of its bioinformatically selected partner lncRNA growth arrest-specific 5 (GAS5) in a sample of Egyptian cancer patients, including three prevalent types of cancer in our region; renal cell carcinoma (RCC), glioblastoma (GB), and hepatocellular carcinoma (HCC) as well as to correlate these expression profiles with the available clinicopathological data in an attempt to clarify their roles in cancer. Quantitative real-time polymerase chain reaction analysis was applied. Different bioinformatics databases were searched to confirm the potential miRNAs-lncRNA interactions of the selected ncRNAs in cancer pathogenesis. The tumor suppressor lncRNA GAS5 was significantly under-expressed in the three types of cancer [0.08 (0.006–0.38) in RCC, $p < 0.001$; 0.10 (0.003–0.89) in GB, $p < 0.001$; and 0.12 (0.015–0.74) in HCC, $p < 0.001$]. However, levels of miR-34a greatly varied according to the tumor type; it displayed an increased expression in RCC [4.05 (1.003–22.69), $p < 0.001$] and a decreased expression in GB [0.35 (0.04–0.95), $p < 0.001$]. Consistent to the computationally predicted miRNA-lncRNA interaction, negative correlations were observed between levels of GAS5 and miR-34a in RCC samples ($r = -0.949$, $p < 0.001$), GB ($r = -0.518$, $p < 0.001$) and HCC ($r = -0.455$, $p = 0.013$). Kaplan-Meier curve analysis revealed that RCC patients with down-regulated miR-34a levels had significantly poor overall survival than their corresponding ($p < 0.05$). Hierarchical clustering analysis showed RCC patients could be clustered by GAS5 and miR-34a co-expression profile. Our results suggest potential applicability of GAS5 and miR-34a with other conventional markers for various types of cancer. Further functional validation studies are warranted to confirm miR-34a/GAS5 interplay in cancer.

Introduction

Cancer is now the second leading cause of mortality worldwide, causing 8.8 million deaths globally in 2015, which is equivalent to one in every six deaths [1]. Cancer occurs as a net result of activation of oncogenes and inhibition of tumor suppressor genes (TSGs) [2]. Decades back, it was believed that oncogenes and TSGs had to code for proteins, and only mutations in protein-coding genes would result in such pathological conditions as cancer. With the advancement of genetic technologies including next generation sequencing, microarrays and bioinformatic machinery, many truths came to light, including what was originally thought to be junk DNA is now found to code for thousands of equally significant regulatory RNAs [3]. Since their discovery, the non-coding RNAs (ncRNAs) have been recognized as epigenetic regulators of protein-coding genes. Recently, a whole new level of regulation has been uncovered; when it was found that ncRNAs have the ability to regulate each other as well [4] further adding to the complexity of the regulatory processes. This set of findings has revolutionized our understanding of several human diseases, making this ‘the era of non-coding RNAs’.

Many classes of ncRNAs have been identified and linked to cancer, the most common of which are micro RNAs (miRNAs), long-noncoding RNAs (lncRNAs), PIWI-interacting RNAs (piRNAs) and small nucleolar RNAs (snoRNAs). The roles of these four types of ncRNAs in cancer are reviewed in several studies [5–8]. In brief, overexpression of some ncRNAs as miRNAs or lncRNAs can suppress the expression of TSG targets, while loss of function or reduced expression of others may allow overexpression of the oncogenes they regulate. Furthermore, since each ncRNA may regulate hundreds of different genes, its over or under expression may have widespread oncogenic effects because many genes will be dysregulated [9].

Here we were interested in a relatively newly discovered lncRNA; Growth Arrest Specific 5 (GAS5) which is a poorly conserved gene mapped to chromosome 1q25.1 [10]. It consists of 12 exons and 11 introns from which 29 transcripts are produced from alternative splicing, many of which contain retained introns (Ensembl Genome Browser ‘GAS5’). The first two transcripts discovered (produced from alternative splice sites on exon 7) are the GAS5a and GAS5b with the latter being predominantly expressed in most cells [11]. Another synonym for the gene is ‘Small Nucleolar RNA Host Gene’, this is for having the ability to produce multiple (10 in human) non-coding small nucleolar RNAs (snRNAs) from its more conserved introns [11]. These snRNAs are involved in the regulation of ribosomal RNA (rRNA) synthesis through 2-O-methylation of pre-ribosomal RNA [12].

As its name implies, GAS5 is over expressed in growth-arrested cells [13]. This is further demonstrated by the presence of high levels of GAS5 in brain cells, which are considered the slowest dividing cells in the body as opposed to its lowest levels in other rapidly dividing cells, the most important of which are cancer cells [14].

Expectedly, GAS5 under expression was found to be associated with multiple types of cancer [15–25] and it was found to bind some miRNAs, including miR-21, miR-222 and miR-103 sponging their inhibitory effect on their target TSGs [16, 21, 26, 27].

Our bioinformatic analyses have revealed a potential new miRNA target for the GAS5 gene; miR-34a. This miRNA is encoded from chromosome 1p36.22. Its promotor is recognized for having multiple CpG islands and a p53 binding site, making p53 a direct transcriptional regulator for this miRNA [28, 29]. While the history of miR-34a with cancer is very well established, studies conducted on different types of cancers have contradictory results regarding its actual role in tumor progression. For instance, many studies have proved it’s functioning as a TSG in various types of cancer, including neuroblastoma [30], leukemia [31], pancreatic [32] and hepatocellular [33, 34] carcinoma, glioblastoma (GB) [35, 36], breast [37] lung [38] and colon [39] cancer. On the contrary, other studies have found that it functions as an oncogene

through promoting tumorigenesis as in RCC [40, 41], papillary thyroid carcinoma (PTC) [42], colon [39] and uterine cancer [43]. It has been suggested that this discrepancy may be attributed to the tissue type and the miR-34a/p53 pathway involved [41].

To the best of our knowledge, no clinical studies were conducted to explore both GAS5 and miR-34a profiles in cancer patients. Hence, we were interested to investigate the expression profiles of these ncRNAs in three prevalent types of cancer in our region; renal cell carcinoma (RCC), hepatocellular carcinoma (HCC) and glioblastoma (GB) as well as to correlate these expression profiles with the available clinicopathological data in an attempt to clarify their roles in cancer.

Materials and methods

Genomic characterization of GAS5 and miR-34a

Chromosomal localization, genomic sequence and structure analysis, subcellular localization, variant analysis, and folding pattern were retrieved from different online tools; including Ensembl (<http://www.ensembl.org/>), GeneCards for human gene database (<http://www.genecards.org/>), National Center for Biotechnology Information (NCBI) (ncbi.nlm.nih.gov/), COMPARTMENTS subcellular localization (<https://compartments.jensenlab.org/Search>), Database of Transcription Start Sites (DBTSS) version 10.0 (<http://dbtss.hgc.jp/>), KineFold (<http://kinfold.curie.fr/>), and MFold webserver (<http://unafold.rna.albany.edu/?q=mfold/RNA-Folding-Form>).

Exploring miR-34 and GAS5 interactions

Identifying complementary regions between microRNA-34a and lncRNA GAS5 were demonstrated by several tools; RNA22 microRNA target detection (<https://cm.jefferson.edu/rna22/>) and DIANA-LncBase v2 (<http://diana.imis.athena-innovation.gr/DianaTools/index.php>).

Functional enrichment analysis

Pathway enrichment analysis and gene ontology of microRNA-34a was performed by Diana-miRPath v3.0 (<http://diana.imis.athena-innovation.gr/DianaTools/index.php>) using its experimentally validated gene targets. Functional enrichment analysis of GAS5 was obtained from Ensembl and GeneCards databases to identify its biological function in cancer.

Study population and sampling collection

In total, 230 samples were analyzed, including 60 formalin-fixed, paraffin-embedded (FFPE) RCC samples and their paired adjacent non-cancer tissues, 50 FFPE GB specimens and 10 non-cancer brain tissues as well as 30 HCC blood samples and 20 controls.

(a) RCC cohort. The archived FFPE renal samples were taken from sixty patients who underwent radical nephrectomy for a primary RCC and dating back for three years. All retrieved cases were archived in the Pathology laboratory of Mansoura Oncology Center, Mansoura, Egypt. No history of receiving neoadjuvant chemotherapy or radiotherapy prior to sampling. Clinicopathological data, including the survival were collected from patient medical records. Paired sixty cancer-free adjacent tissues were examined and sectioned to serve as controls for molecular analysis.

(b) GB cohort. Fifty glioblastoma patients and 10 non-cancer brain tissues collected from the archive of the Pathology Department, Mansoura University Hospitals, Egypt, dating back for three years were included in the current work. Detailed patients' data were retrieved from

their follow up records. They had GB grade 4, undergone surgical removal and had not received any treatment before sampling. They followed-up for more than 3 years.

(c) HCC cohort. Following our local hospital and medical ethical committee rules in liver tissue sampling prohibition from HCC patients, only blood samples were available. Thirty HCV-induced HCC and 20 matched controls from healthy blood bank donors were recruited in the study. Patients were obtained from the outpatient clinic of Tropical Medicine and Gastroenterology Department, Faculty of Medicine, Assuit, Egypt. They had typical imaging findings of liver cancer and elevated alpha fetoprotein (AFP). Patients underwent clinical and radiological assessment, confirmation of HCV by PCR, Barcelona-Clinic Liver Cancer (BCLC) staging, and Child-Turcotte-Pugh (CTP) scoring [44]. Survival data for HCC patients were not available in patients' medical records. Hence, these data were not included in the statistical analysis for HCC patients.

Ethical approval

The study was conducted according to the ethical guidelines of the Declaration of Helsinki and approved by the Medical Research Ethics Committee of Suez Canal University, Faculty of Medicine.

RNA extraction

Total RNA; including the small RNA, was isolated from either FFPE tissue sections (5 to 8- μ m-thick) using the Qiagen miRNeasy FFPE Kit (Qiagen, cat no. 217504) or serum using Qiagen miRNeasy serum/plasma Kit (Qiagen, cat no 217184) following the protocols supplied by the manufacturer. Concentration of RNA was determined using the NanoDrop ND-1000 spectrophotometer (NanoDrop Tech., Inc. Wilmington, DE, USA). Samples with a 260/280 nm absorbance ratio less than 1.8 were excluded.

Reverse transcription reaction

Subsequently, RNA for lncRNA GAS5 was converted to complementary DNA (cDNA) in a T-Professional Basic, Biometra PCR System (Biometra, Goettingen, Germany) using high Capacity cDNA Reverse Transcription Kit (Applied Biosystems, P/N 4368814) with RT random primers as previously described [45].

Reverse transcription of miR-34a was specifically converted to cDNA using TaqMan MicroRNA Reverse Transcription kit (P/N 4366596; Applied Biosystems, Foster City, CA, USA) with 5x miRNA specific stem-loop primers as previously described in our prior publication [46]. Appropriate controls were included in each experiment.

LncRNA GAS5 and microRNA-34a expression analyses

The Real-Time PCR reactions were performed in accordance with the Minimum Information for Publication of Quantitative Real-Time PCR Experiments (MIQE) guidelines [47]. The expression level of GAS5 was assessed via SYBR Green qPCR analysis and normalized with GAPDH in liver, renal, and brain cancer samples. The following primers were designed using Primer 3 software and checked by *in silico* PCR amplification of the University of California, Santa Cruz (UCSC) genome browser; for GAS5: Forward: 5' - CTTGCCTGGACCAGCTTAAT-3'; Reverse: 5' - CAAGCCGACTCTCCATACCT-3', and for GAPDH: Forward: 5' - CCGATTTGGTCGTATTGGG-3'; Reverse: 5' - CTGGAAGATGGTGATGGGATT-3'. In brief, 10 μ l of qPCR Green Master (Jena Bioscience, Cat no. PCR-313L), 0.6 μ l (10 μ M) forward and reverse primers, 8 μ l PCR grade water, and 1 μ l cDNA template were included in the reaction for

GAS5 and *GAPDH* SYBR Green assay analyses [45, 46]. For microRNA quantification, a final volume of 20 μ l was adjusted in duplicate, including 1.33 μ l specific RT products, 2 \times TaqMan Universal PCR Master Mix with UNG (Applied Biosystems, P/N 4440043), and 20 \times of 1 μ l specific TaqManRNA assay for hsa-miR-34a-5p (Applied Biosystems, assay ID 000426) compared to the endogenous control RNU6B (assay ID Hs001093) [48]. Three other endogenous control assays were used in brain cancer [49, 50] and TATA box binding protein (*TBP*; TaqMan assay ID Hs00427620_m1) replaced *GAPDH* for normalization based on our prior work which showed its consistency across samples [36]. Appropriate negative and positive controls were used. A negative control without template was included in each run to exclude contamination of PCR product with genomic DNA. Positive control samples were reapplied in each experiment to test the quality and consistency of the PCR reaction. The PCR for 96-well plates was carried out using StepOne Real-Time PCR System (Applied Biosystem) and incubated as follows: 95°C for 10 min followed by 45 cycles of 92°C for 15 seconds and 60°C for 1 minute. Ten percent randomly selected study samples were re-evaluated in separate runs for the study gene expressions to test the reproducibility of the qPCR which showed very close quantitative cycle value results and low standard deviations.

Statistical analysis

R package (version 3.3.2) and Statistical Package for the Social Sciences (SPSS) for Windows software (version 23.0) were used for data analyses. Categorical variables were compared using the Chi-square (χ^2) or Fisher's exact tests where appropriate. Wilcoxon matched-pair signed-rank and Mann-Whitney U tests were used for tissues of renal/brain cancer and serum of liver cancer patients, respectively, to compare continuous variables. The correlation between miR-34a level and *GAS5* expressions was calculated by Spearman's rank correlation analysis. A two-tailed *p*-value of < 0.05 was considered statistically significant. The receiver operating characteristic (ROC) curves were performed to get the best cutoff values of miRNA-34a for discriminating long and short survivors in cancer patients. The fold change of ncRNAs expressions in each patient relative to the control was calculated via Livak method based on the quantitative cycle (C_q) values with the following equation: relative quantity = $2^{-\Delta\Delta C_q}$, where $\Delta\Delta C_q = (C_q \text{ ncRNA} - C_q \text{ internal control})_{\text{cancer}} - (C_q \text{ ncRNA} - C_q \text{ internal control})_{\text{control}}$ [51]. Univariate analysis for association between ncRNA expression profile and clinico-pathological features in cancer patients was run. The software package named PC-ORD version 6 [52] was employed to run different multivariate analyses for clustering analysis of patients according to clinico-pathological and molecular data.

Results

Genomic location of GAS5

Lnc-RNA GAS5 is also known as small nucleolar RNA host gene 2 (SNHG2) and non-protein coding RNA 30 (NCRNA00030). It is encoded by *GAS5* gene on chromosome 1q25.1 (Genomic coordination at 1:173863901–173867987 at the negative strand according to human genome assembly GRCh38) (Fig 1A). It consists of 12 exons, spanning 4.087 kb and encoding for 29 different alternative splice transcripts ranging in length from 242 to 1698 bp (S1 Table).

Sequence analysis of GAS5

GAS5 gene contains a seven-nucleotide oligo-pyrimidine tract on its 5'-end in exon 1, hence is classified as a member of the 5' terminal oligo-pyrimidine (TOP) genes. This sequence can act as a cis-regulatory motif which either inhibits the binding of translational regulatory proteins

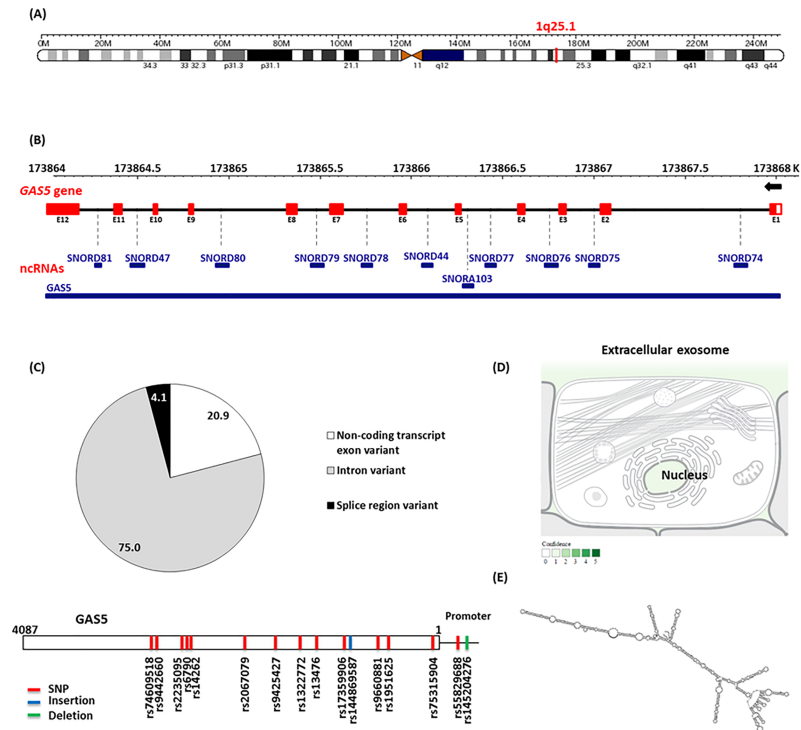


Fig 1. Structural analysis of GAS5 gene. (A) Chromosomal localization of GAS5 gene. It is present on chromosome 1q25.1, at genomic coordination 1:173863901–173867987 on the negative strand (according to human genome assembly GRCh38). (B) Sequence analysis of GAS5 gene. It consists of 12 exons, spanning 4.087 kb that code for 29 different alternative splice transcripts. It hosts multiple snoRNA genes within its introns (except intron 9). These genes encode for ten C/D box snoRNAs, which contain the C (UGAUGA) and D (CUGA) box motifs, and an H/ACA box snoRNA, SNORDA103, within intron 4. (C) Genetic variant analysis. GAS5 gene (4087 bases long) contains around 300 thousand variants (75% intronic, 21% exonic, and 4% splice region polymorphisms). Among all these polymorphisms, 14 SNPs (red), one deletion (green) and one insertion (blue) are common variants with minor allele frequency (MAF) > 0.05. (D) Subcellular localization of lncRNA GAS5. Text mining highlighted its predominant existence intranuclear and within extracellular exosomes which are extruded into the circulation. (E) Folding pattern of lncRNA GAS5. [Data source: Ensembl.org, genecards.org, NCBI, COMPARTMENT database, and MFold].

<https://doi.org/10.1371/journal.pone.0198231.g001>

downstream to the transcriptional start sites of mRNAs or suppresses the translational machinery itself. In addition to its translational controls, the TOP elements are known to modulate gene expression through regulating transcription [53]. Being one of the TOP genes, it is ubiquitously expressed and is predicted to regulate the translation of more than 20% of total mRNAs [DataBase of Transcription Start Sites]

Sequence analysis of GAS5 gene revealed that it is a small nucleolar RNA host gene, containing multiple *snoRNA* genes within its introns. These genes encode for ten C/D box snoRNAs, which contain the C (UGAUGA) and D (CUGA) box motifs. They are predicted to play a role in the 2'-O-methylation of rRNA by guiding guanine methylation, which enhances RNA folding and interaction with ribosomal proteins. GAS5 also hosts SNORDA103 within intron 4, an H/ACA box snoRNA, which is associated with pseudouridylation (Fig 1B).

Variant analysis

GAS5 gene is shown to be highly polymorphic, enclosing around 300 thousand variants (75% intronic, 21% exonic, and 4% splice region polymorphisms). Among all these polymorphisms, 14 SNPs, one deletion and one insertion are common variants with minor allele frequency (MAF) > 0.05 (Fig 1C) and (S2 Table).

GAS5-miRNA interaction

Analysis with the RNA22 program (<http://cbcsrv.watson.ibm.com/rna22.html>) identified complementary regions of GAS5 with 690 microRNAs. Among these putative microRNAs, only 252 interactions with 234 microRNAs showed significant binding ($p < 0.05$) (S3 Table). Via DIANA-LncBase v2 database for experimentally validated miRNA-lncRNA interactions, GAS5 was identified as a miR-34a target by immunoprecipitation experiments (score = 0.558). For further confirmation, we used RNA22 software to determine the interaction binding sites between GAS5 transcripts and miR-34a. Our results showed base-pairing in twenty-three alternative splice variants. Among them, nine transcripts had two miR-34a binding sites (S4 Table).

miR-34a functional analysis. Hundreds of miR-34a-5p and 3p targets were retrieved from various online databases; including miRTarBase (<http://mirtarbase.mbc.nctu.edu.tw/>), miRDB (<http://mirdb.org/>) and microRNA.org. Functional enrichment analysis revealed its enrollment in cancer-related KEGG pathways, as Pathways in cancer (hsa05200, 115 targets, $p = 0.001723304$), proteoglycans in cancer (hsa05205, 71 targets, $p = 1.687731e-06$), adherens junction (hsa04520, 34 targets, $p = 3.396929e-06$), cell cycle (hsa04110, 54 targets, $p = 3.355808e-05$), and p53 signaling pathway (hsa04115, 31 targets, $p = 0.006060223$) as well as cancer-specific pathways, namely glioma (hsa05214, 29 targets, $p = 0.0003111577$) and renal cell carcinoma (hsa05211, 28 targets, $p = 0.02521455$) (S5 Table). GO analysis (Diana tools) demonstrated miR-34a to be involved in cell death, cell cycle, and response to stress thus highlighting its role in cancer cell growth. In addition, miR-34a was significantly associated with membrane organization, cell junction organization, and cell motility, hence may play a key role in cancer cell invasion and metastasis (Fig 2).

Characteristics of the study population

Baseline characteristics of RCC, GB, and HCC cohorts are demonstrated in Tables 1–3.

Expression profiling

GAS5 levels were under-expressed in RCC [0.08 (0.006–0.38), $p < 0.001$], GB [0.10 (0.003–0.89), $p < 0.001$] and HCC [0.12 (0.015–0.74), $p < 0.001$]. On the other hand, miR-34a displayed an increased expression in RCC [4.05 (1.003–22.69), $p < 0.001$] and a decreased expression in GB [0.35 (0.04–0.95), $p < 0.001$] as depicted in Fig 3. Aligned with the computationally predicted interaction between microRNA and lncRNA in our bioinformatics analysis, a very strong correlation between the expression profile of GAS5 and miR-34a was detected in RCC samples [$r = -0.949$, $p < 0.001$] and a moderate negative correlation was observed between levels of GAS5 and miR-34a in GB [$r = -0.518$, $p < 0.001$] and HCC [$r = -0.455$, $p = 0.013$] (Fig 4).

Association of GAS5 and miR-34a with clinicopathological features

Univariate analyses are shown in Table 4A, 4B and 4C. ROC curves showed no prognostic value for GAS5 nor miR-34a to predict survival of cancer patients in RCC and GB, or to predict CTP class for liver cell failure in HCC patients ($p > 0.05$) (S1 Fig).

Survival analysis in RCC and GB

In RCC, multivariable analysis using logistic regression test (Enter method) showed age and pathological grade to be independent predictors for recurrence: (OR = 1.251, 95% CI = 1.075–1.455, $p = 0.004$) for the age and (OR = 19.9, 95% CI = 1.034–383, $p = 0.047$) for the grade. Kaplan-Meier curve analysis and log-rank test revealed that RCC patients with female gender,

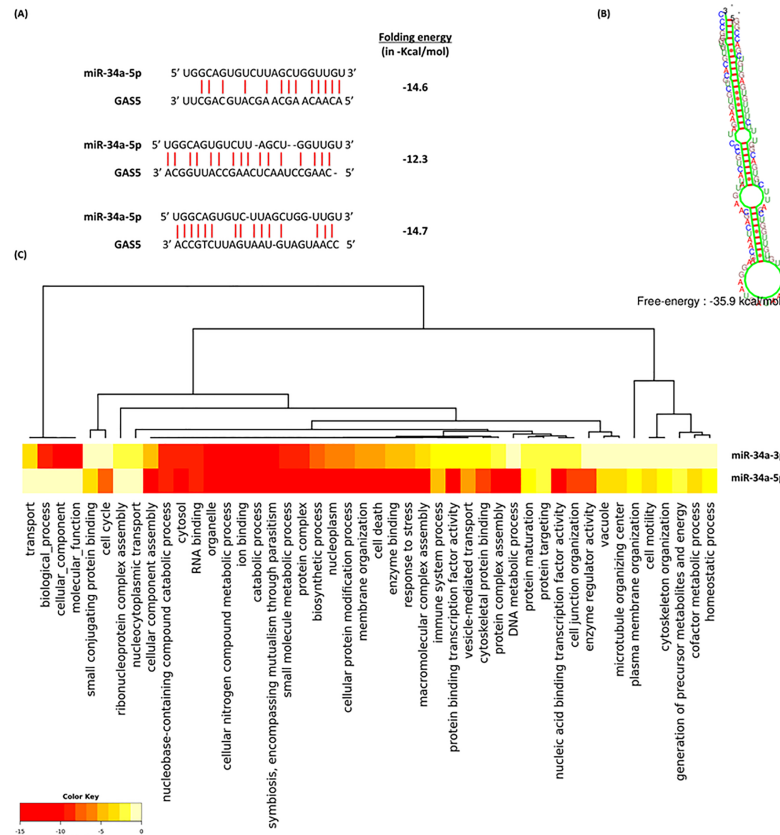


Fig 2. Functional and structural analysis of miR-34a. (A) GAS5: miR-34a-5p interaction. Complementarity regions are shown in three binding sites in GAS5 gene, one proximal at 5' region (1432–1455) and two distal at 3' end (3545–3567 and 3698–3719) [Data source: RNA22, DIANA-LncBase v2]. (B) Predicted secondary structure of miR-34a. Folding pattern and energy are demonstrated [Data source: KineFold]. (C) Functional enrichment analysis of miR-34a experimentally validated gene targets. Significant clustered heat map represents the gene ontology using GO slim option, FDR conservative states, *p* value threshold < 0.05, and categories union [Data source: DIANA-miRPath v3]. <http://snf-515788.vm.okanos.grnet.gr/#mirnas=hsa-miR-34a-3p;hsa-miR-34a-5p&methods=Tarbase;Tarbase&selection=2>.

<https://doi.org/10.1371/journal.pone.0198231.g002>

post-nephrectomy recurrence, advanced pathological grade, and down-regulated miR-34a levels had significantly poor overall survival than their corresponding ($p < 0.05$) (Table 5). In addition, multivariable analysis by Cox regression model demonstrated sex and the recurrence to be independent predictors of overall survival (hazard ratio (HR) = 2.49; 95% confidence interval (95% CI) 1.14–5.41, $p = 0.021$) and (HR = 4.16; 95% CI of 1.88–9.16, $p < 0.001$), respectively.

In GB, Kaplan-Meier curves showed a significant association of shorter survival times with male gender (Breslow test: $p = 0.002$ and Tarane-Ware test: $p = 0.030$). In addition, marginal significance was observed for poor overall survival in patients with frontal lesions (Log rank test: $p = 0.050$) (Table 6). Multivariable analysis by Cox regression model illustrated tumor recurrence to be an independent predictor of low overall survival (HZ = 11.1; 95% CI 2.88–42.5, $p < 0.001$).

Hierarchical clustering analysis

Dendrograms for Two-way agglomerative hierarchical cluster analysis were employed for data exploration (Fig 5). The following cluster setup parameters were adjusted: Distance method:

Table 1. Clinicopathological characteristics of renal cell carcinoma patients.

| Variables | Total | Low OS | High OS | p value |
|-----------------------|-----------|-----------|-----------|------------------|
| Total number | 60 (100) | 19 (31.7) | 41 (68.3) | |
| Age | | | | |
| ≤55 years | 6 (10.0) | 3 (15.8) | 3 (7.3) | 0.370 |
| >55 years | 54 (90.0) | 16 (84.2) | 38 (92.7) | |
| Sex | | | | |
| Female | 21 (35.0) | 9 (47.4) | 1 (29.3) | 0.245 |
| Male | 39 (65.0) | 10 (52.6) | 29 (70.7) | |
| HPD | | | | |
| Clear cell | 30 (50.0) | 8 (42.1) | 22 (53.7) | 0.354 |
| Papillary | 15 (25.0) | 4 (21.1) | 11 (26.8) | |
| Chromophobic | 15 (25.0) | 7 (36.8) | 8 (19.5) | |
| Tumor location | | | | |
| Right side | 22 (36.7) | 7 (36.8) | 15 (36.6) | 0.985 |
| Left side | 38 (63.3) | 12 (63.2) | 26 (63.4) | |
| Grade | | | | |
| Grade 1 | 9 (15.0) | 1 (5.3) | 8 (19.5) | 0.023 |
| Grade 2 | 28 (46.7) | 6 (31.6) | 22 (53.7) | |
| Grade 3 | 23 (38.3) | 12 (63.2) | 11 (26.8) | |
| Tumor size | | | | |
| T1 | 21 (35.0) | 6 (31.6) | 15 (36.6) | 0.589 |
| T2 | 25 (41.7) | 7 (16.8) | 18 (43.9) | |
| T3 | 14 (23.3) | 6 (31.6) | 8 (19.5) | |
| LN | | | | |
| Negative | 39 (65.0) | 11 (57.9) | 28 (68.3) | 0.562 |
| Positive | 21 (35.0) | 8 (42.1) | 13 (31.7) | |
| Recurrence | | | | |
| Negative | 44 (73.3) | 7 (36.8) | 37 (90.2) | <0.001 |
| Positive | 16 (26.7) | 12 (63.2) | 4 (9.8) | |
| DFS | | | | |
| ≤ 1year | 29 (48.3) | 19 (100) | 10 (24.4) | <0.001 |
| > 1year | 31 (51.7) | 0 (0.0) | 31 (75.6) | |
| GAS5 fold | | | | |
| ≤ 1-fold | 55 (91.7) | 19 (100) | 36 (87.8) | 0.283 |
| > 1-fold | 3 (5.0) | 0 (0.0) | 3 (7.3) | |
| >10-folds | 2 (3.3) | 0 (0.0) | 2 (4.9) | |
| miR-34a fold | | | | |
| ≤ 1-fold | 15 (25.0) | 6 (31.6) | 9 (22.0) | 0.192 |
| > 1-fold | 19 (31.7) | 8 (42.1) | 11 (26.8) | |
| >10-folds | 26 (43.3) | 5 (26.3) | 21 (51.2) | |

HPD histopathological diagnosis, DFS disease-free survival, OS overall survival. Low OS: ≤12 months, High OS: >12 months. Fisher’s Exact and Pearson Chi-square tests were used. Bold values indicate statistical significance at $p < 0.05$

<https://doi.org/10.1371/journal.pone.0198231.t001>

Sorensen (Bray-Curtis), Group Linkage Method: Flexible Beta at 0.75, Clustering of factor relative by factor maximum. A distance matrix is shown. RCC plot analyzed 60 strands and 12 factors, GB plot analyzed 50 strands and 9 factors, whereas HCC dendrogram showed results of 30 strands and 11 factors. Clustering analysis revealed separation of RCC patients by GAS5

Table 2. Clinicopathological characteristics of glioblastoma patients.

| Variables | Total | Low OS | High OS | p value |
|-----------------------|-----------|-----------|-----------|--------------|
| Total number | 50 (100) | 10 (20.0) | 40 (80.0) | |
| Age | | | | |
| ≤55 years | 21 (42.0) | 7 (70.0) | 14 (35.0) | 0.073 |
| >55 years | 29 (58.0) | 3 (3.0) | 26 (65.0) | |
| Sex | | | | |
| Female | 13 (26.0) | 1 (10.0) | 12 (30.0) | 0.258 |
| Male | 37 (74.0) | 9 (90.0) | 28 (70.0) | |
| Tumor location | | | | |
| Frontal | 24 (48.0) | 8 (80.0) | 16 (40.0) | 0.071 |
| Temporo-paroetal | 18 (36.0) | 1 (10.0) | 17 (42.5) | |
| Fronto-temporal | 8 (16.0) | 1 (10.0) | 7 (17.5) | |
| Recurrence | | | | |
| Negative | 44 (88.0) | 8 (80.0) | 36 (90.0) | 0.586 |
| Positive | 6 (12.0) | 2 (20.0) | 4 (10.0) | |
| DFS | | | | |
| ≤ 1year | 25 (50.0) | 10 (100) | 15 (37.5) | 0.001 |
| > 1year | 25 (50.0) | 0 (0.0) | 25 (62.5) | |
| GAS5 fold | | | | |
| ≤ 1-fold | 37 (74.0) | 7 (70.0) | 30 (75.0) | 0.707 |
| > 1-fold | 13 (26.0) | 3 (30.0) | 10 (25.0) | |
| >10-folds | | | | |
| miR-34a fold | | | | |
| ≤ 1-fold | 38 (76.0) | 8 (80.0) | 30 (75.0) | 0.741 |
| > 1-fold | 12 (24.0) | 2 (20.0) | 10 (25.0) | |
| >10-folds | 0 (0.0) | | | |

Data are presented as number (frequency). *HPD* histopathological diagnosis, *DFS* disease-free survival, *OS* overall survival. Low OS: ≤12 months, High OS: >12 months. Fisher’s Exact and Pearson Chi-square tests were used. Bold values indicate statistical significance at $p < 0.05$

<https://doi.org/10.1371/journal.pone.0198231.t002>

and miR-34a levels, GB patients by survival times, and HCC patients by their age. However, it is worth noting that Cox regression analysis is more accurate and specific for survival analysis, while the purpose of multivariate analysis is to graphically expose the relationship between cluster analyses and individual data points, making it easy to see similarities and differences between patients of the same cancer types.

Discussion

In this study, we measured the expression of two ncRNAs; the lncRNA GAS5 and the miRNA miR-34a in three of the most prevalent and high-incidence tumors in Egypt; hepatic, renal and brain cancer. We chose more than one tumor type to assess if the same ncRNA could work differently according to the tissue type. We also investigated the possible association between GAS5 and miR-34a in mediating carcinogenesis after detecting an interaction between the two through our preliminary *in silico* analysis.

Our results show that GAS5 was under-expressed in the three types of cancer; RCC, HCC and GB. On the other hand, levels of miR-34a greatly varied according to the tumor type. RCC patients had a lower GAS5 level and a higher miR-34a level in tumor tissue compared to adjacent non-cancer tissue. In accordance, Qiao et al. reported a reduced GAS5 level in RCC cell

Table 3. Clinicopathological characteristics of hepatocellular carcinoma patients.

| Variables | Patients (n = 30) |
|--------------------------|-------------------|
| Total number | |
| Age | |
| ≤55 years | 13 (43.3) |
| >55 years | 17 (56.7) |
| Sex | |
| Female | 11 (36.7) |
| Male | 19 (63.3) |
| Tumor size | |
| <5 cm | 9 (30.0) |
| ≥5 cm | 21 (70.0) |
| Number of lesions | |
| Solitary | 20 (66.7) |
| Multiple | 10 (33.3) |
| LCF score | 9.7±1.2 |
| CTP class | |
| Child B | 21 (70.0) |
| Child C | 9 (30.0) |
| Hepatomegaly | |
| Mild | 18 (60.0) |
| Massive | 12 (40.0) |
| Treatment | |
| Ablation | 15 (30.0) |
| Radiofrequency | 11 (36.7) |
| Supportive | 4 (13.3) |
| GAS5 fold | |
| ≤ 1-fold | 27 (90.0) |
| > 1-fold | 3 (10.0) |
| miR-34a fold | |
| ≤ 1-fold | 19 (63.3) |
| > 1-fold | 10 (33.3) |

Data are presented as number (frequency). CTP Child-Turcotte-Pugh classification for liver cell failure, LCF liver cell failure score by CTP classification. Fisher’s Exact and Pearson Chi-square tests were used.

<https://doi.org/10.1371/journal.pone.0198231.t003>

lines compared to normal cell lines. Furthermore, in *vitro* cloning and functional expression analysis revealed that GAS5 overexpression caused cell cycle arrest, increased apoptosis, as well as inhibited tumor metastatic potential [24], which could explain the correlation between reduced patient survival and GAS5 level in our study. As for miR-34a, several studies reported over-expression of this RNA in RCC patients [40, 41, 54–56]. Liu et al. predicted that its oncogenic function could be through targeting the two tumor suppressors secreted frizzled related protein 1 (SFRP1) and calmodulin binding transcription activator 1 (CAMTA1), and further validated the first target [40]. Another study noticed that miR-34a enhances cell survival, both in *vitro* and in *vivo* during cisplatin nephrotoxicity through p53 [57]. Collectively, the previous studies suggest that miR-34a can act as an oncogene in renal tissue. On the contrary, Yadav et al. detected a significant under-expression of miR-34a in both sera and renal tissues of RCC patients [58]. Similar results were demonstrated by the studies of Zhang et al. and Weng et al. [59, 60], where the former study demonstrated that decreased expression of miR-34a in RCC

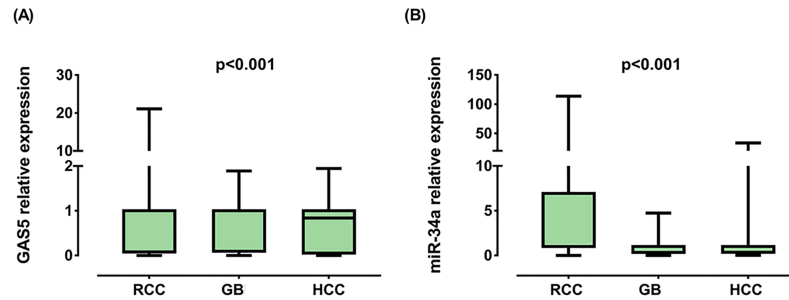


Fig 3. Relative expression of GAS5 and miR-34a-5p in cancer. RCC renal cell carcinoma, GB glioblastoma, HCC hepatocellular carcinoma. Data are represented as medians. The box defines upper and lower quartiles (25% and 75%, respectively) and the error bars indicate upper and lower adjacent limits. Expression levels in cancer and control samples were normalized to GAPDH in RCC and HCC, TBP in GB and RNU6B for microRNA and calculated using the delta-delta CT method [$= 2^{(-\Delta\Delta CT)}$] in comparison to controls. Fold change of controls were set at 1.0. Wilcoxon matched-pair signed-rank and Mann-Whitney U tests were used for tissues of renal/brain cancer and serum of liver cancer patients, respectively. Two-sided $p < 0.05$ was considered statistically significant.

<https://doi.org/10.1371/journal.pone.0198231.g003>

patients inversely up-regulated the gene for the transcription factor YY1. The latter study suggested that under-expression of miR-34a in cancer tissues of RCC patients affected the regulation of the *NOTCH1* gene, as well as caused dysregulation of other multiple miR-34a targets in 786-O and Caki-1 RCC cell lines. Yu et al. found that miR-34a suppressed tumor growth and metastasis *in vivo* and *in vitro* through targeting CD44 [61]. Another study found that miR-34a inhibits cellular invasion in renal cancer cell lines A498 and 769P through targeting the 3' untranslated region (UTR) of the *c-myc* oncogene [62]. Also, the lncRNA NEAT1 (nuclear paraspeckle assembly transcript 1) was found to sponge miR-34a releasing its inhibition on the *c-met* oncogene, resulting in increased cellular proliferation and invasion in RCC cell lines 786-O and ACHN [63]. Furthermore, Bai et al. found that miR-34a causes senescence of rat renal cells through targeting two anti-oxidative mitochondrial genes [64]. Cellular senescence, which is an irreversible state of growth arrest, protects the cells from accumulating mutations that could lead to malignant transformation [65]. Further supporting the tumor suppressor potential of miR-34a, Zhou et al. provided evidence that miR-34a, secreted by fibroblasts, enhances apoptosis of renal tubular cells through regulating the anti-apoptotic gene *BCL-2* [66].

The inconsistent results between our study which shows up-regulation of *miR-34a* in RCC and other studies showing its under-regulation in the same type of cancer could have many

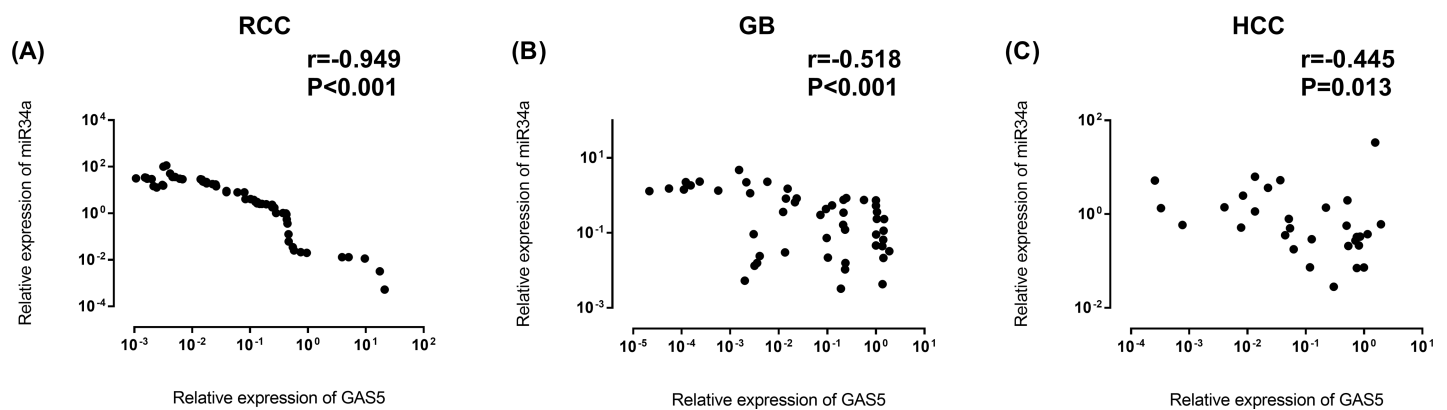


Fig 4. Correlation between GAS5 and miR-34a-5p expression levels. RCC renal cell carcinoma, GB glioblastoma, HCC hepatocellular carcinoma. Data were log transformed. Spearman's rank correlation test was used. Statistical significance was considered at $p < 0.05$.

<https://doi.org/10.1371/journal.pone.0198231.g004>

Table 4. Univariate analysis for association between gene profile and clinico-pathological features in the study cohorts.

| | (a) RCC | | | |
|-------------------|-------------------------|---------------------------------------|-------------------------|---------------------------------------|
| | GAS5 | | miR-34a | |
| | <i>p</i> _{ass} | <i>r</i> (<i>p</i> _{corr}) | <i>p</i> _{ass} | <i>r</i> (<i>p</i> _{corr}) |
| Age | 0.239 | -0.069 (0.598) | 0.352 | -0.066 (0.619) |
| Sex | 0.631 | 0.063 (0.635) | 0.798 | -0.033 (0.801) |
| Location | 0.908 | -0.015 (0.910) | 0.884 | 0.019 (0.886) |
| HPD | 0.257 | 0.191 (0.143) | 0.504 | -0.130 (0.321) |
| Grade | 0.402 | 0.171 (0.192) | 0.378 | -0.167 (0.204) |
| Tumor size | 0.199 | 0.157 (0.230) | 0.361 | -0.152 (0.246) |
| LN | 0.193 | 0.169 (0.195) | 0.258 | -0.147 (0.261) |
| Recurrence | 0.192 | 0.170 (0.195) | 0.371 | -0.116 (0.376) |
| DFS | 0.120 | 0.305 (0.018) | 0.363 | 0.215 (0.099) |
| OS | 0.266 | 0.283 (0.029) | 0.441 | 0.191 (0.144) |
| | (b) GB | | | |
| Age | 0.883 | 0.063 (0.663) | 0.930 | -0.013 (0.931) |
| Sex | 0.921 | -0.014 (0.922) | 0.514 | -0.093 (0.520) |
| Location | 0.530 | -0.150 (0.300) | 0.711 | 0.091 (0.531) |
| Recurrence | 0.258 | 0.166 (0.248) | 0.070 | -0.260 (0.068) |
| DFS | 0.869 | 0.012 (0.936) | 0.677 | 0.074 (0.609) |
| OS | 0.451 | 0.48 (0.743) | 0.356 | 0.013 (0.927) |
| | (c) HCC | | | |
| Age | 0.869 | -0.037 (0.848) | 0.059 | -0.289 (0.121) |
| Sex | 0.553 | 0.112 (0.556) | 0.420 | 0.156 (0.411) |
| Hepatomegaly | 0.692 | -0.079 (0.680) | 0.851 | 0.039 (0.837) |
| Tumor size | 0.226 | 0.278 (0.137) | 0.209 | -0.315 (0.090) |
| Number of lesions | 0.193 | -0.352 (0.056) | 0.916 | 0.112 (0.225) |
| CTP class | 0.283 | -0.206 (0.275) | 0.533 | 0.122 (0.521) |
| Treatment | 0.715 | 0.144 (0.447) | 0.598 | 0.006 (0.973) |

*p*_{ass} *p* values for association, *r* (*p*_{corr}) correlation spearman’s coefficient and *p* value of correlation, *HPD* histopathological diagnosis, *T* tumor size, *LN* lymph node, *DFS* disease-free survival, *OS* overall survival, *CTP* Child-Turcotte-Pugh classification for liver cell failure. Spearman’s rank, Mann-Whitney U and Kruskal-Wallis tests were used. Statistically significant values (*p* < 0.05) are shown in bold.

<https://doi.org/10.1371/journal.pone.0198231.t004>

possible explanations. First, we measured the expression of miR-34a in cancer tissues obtained directly from RCC patients as opposed to other studies conducted on cancer cell lines. While those cell lines are highly essential for functional molecular analysis, they may be different from primary tumors, possibly through building up new mutations in their attempt to adjust to their artificial environment [67, 68]. Such mutations may easily alter cellular responses and regulatory mechanisms, possibly affecting the expression of *miR-34a*. Second, miR-34a could be a non-specific molecule that can both activate or inhibit tumorigenesis depending on the surrounding environment. These include internal stimuli (other regulatory molecules or polymorphisms, oxidative molecules, other associated disease states, tumor stage/grade or else) and external stimuli (cellular response to environmental exposures, including chemotherapy, other drugs, chemicals, foods, etc). Third, miR-34a has multiple targets (discussed in our previous work) [41], as well as being itself a target for many lncRNAs. Each study focuses on one or few targets and infers a tumor suppressor or an oncogenic function based on its effect on the studied target/pathway. However, miR-34a is one small molecule in a larger network of molecules that either promotes or inhibits tumorigenesis based on the net result of all its

Table 5. Multivariable analysis in renal cell carcinoma patients.

| Variables | Survival time OS (mo) | Overall comparisons | | | Cox regression | |
|---------------------|--------------------------|---------------------|------------------|------------------|-------------------------|------------------|
| | | Log Rank | Breslow | Tarone-Ware | HR (95% CI) | p |
| Age | | | | | | |
| ≤55 years | 13.1 ± 2.22 | | | | | |
| >55 years | 16.1 ± 0.8 | 0.186 | 0.244 | 0.221 | 0.97 (0.92–1.01) | 0.217 |
| Sex | | | | | | |
| Female | 13.9 ± 1.28 | | | | | |
| Male | 16.7 ± 0.94 | 0.027 | 0.077 | 0.095 | 2.49 (1.14–5.41) | 0.021 |
| HPD | | | | | | |
| Type 1 | 16.1 ± 1.12 | | | | | |
| Type 2 | 17.5 ± 1.61 | | | | 0.70 (0.34–1.46) | 0.351 |
| Type 3 | 13.3 ± 1.25 | 0.103 | 0.198 | 0.159 | 0.69 (0.30–1.60) | 0.397 |
| Location | | | | | | |
| Right side | 16.3 ± 1.23 | | | | | |
| Left side | 15.4 ± 1.00 | 0.703 | 0.489 | 0.539 | 1.08 (0.57–2.06) | 0.807 |
| Grade | | | | | | |
| Grade 1 | 16.3 ± 1.53 | | | | | |
| Grade 2 | 18.0 ± 1.17 | | | | | |
| Grade 3 | 12.8 ± 1.05 | 0.005 | 0.003 | 0.003 | 1.60 (0.66–3.85) | 0.293 |
| Tumor size | | | | | | |
| T1 | 16.4 ± 1.40 | | | | | |
| T2 | 15.9 ± 1.13 | | | | 0.91 (0.30–2.75) | 0.871 |
| T3 | 14.5 ± 1.65 | 0.709 | 0.577 | 0.635 | 0.89 (0.34–2.29) | 0.813 |
| LN | | | | | | |
| Negative | 16.4 ± 0.97 | | | | | |
| Positive | 14.6 ± 1.27 | 0.306 | 0.235 | 0.255 | 1.05 (0.42–2.59) | 0.911 |
| Recurrence | | | | | | |
| Negative | 17.5 ± 0.83 | | | | | |
| Positive | 10.8 ± 1.07 | <0.001 | <0.001 | <0.001 | 4.16 (1.88–9.16) | <0.001 |
| GAS5 fold | | | | | | |
| Under-expressed | 15.7 ± 0.84 | | | | | |
| Over-expressed | 16.2 ± 1.24 | 0.735 | 0.753 | 0.985 | 0.29 (1.04–0.96) | 0.291 |
| miR-34a fold | | | | | | |
| Under-expressed | 13.2 ± 0.99 | | | | | |
| Over-expressed | 16.6 ± 0.95 | 0.010 | 0.049 | 0.024 | 1.001 (0.98–1.01) | 0.926 |

Survival times is shown as mean and standard error, OS overall survival, HR (95% CI) Hazard ratio (95% confidence interval), HPD histopathological diagnosis, T tumor size, LN lymph node. Statistically significant values ($p < 0.05$) are shown in bold.

<https://doi.org/10.1371/journal.pone.0198231.t005>

regulated targets, which could easily differ according to countless variables. Given by the negative correlation of this microRNA with GAS5 in our RCC patients, as well as the predicted interaction between the two, we believe that a new pathway; the GAS5/miR-34a pathway might be involved in the previously indicated molecular network leading to RCC.

The interaction between lncRNAs and miRNAs can be multifaceted. Yoon et al. explained four mechanisms of interaction between the two types [69]. First, lncRNAs can act as miRNA sponges as previously mentioned with examples in the introduction. Second, the opposite can occur, where miRNAs can inhibit lncRNAs by binding to them and causing their degradation. This applies for miR145-5p, miR-181a-5p and miR-99b-3p which inhibit lncRNA ROR [70],

Table 6. Multivariable analysis in glioblastoma patients.

| Variables | Survival time OS (mo) | Overall comparisons | | | Cox regression | |
|-----------------------|--------------------------|---------------------|--------------|--------------|-------------------------|------------------|
| | | Log Rank | Breslow | Tarone-Ware | HR (95% CI) | p |
| Age | | | | | | |
| ≤55 years | 17.8 ± 1.4 | 0.742 | 0.683 | 0.595 | 1.03 (0.97–1.09) | 0.298 |
| >55 years | 17.0 ± 0.96 | | | | | |
| Sex | | | | | | |
| Female | 20.5 ± 1.5 | 0.096 | 0.002 | 0.030 | 1.36 (0.45–4.11) | 0.583 |
| Male | 16.2 ± 0.8 | | | | | |
| Tumor location | | | | | | |
| Frontal | 15.7 ± 1.01 | 0.050 | 0.079 | 0.062 | | 0.749 |
| Temporo-paroetal | 17.6 ± 1.3 | | | | 1.3 (0.53–3.39) | 0.534 |
| Fronto-temporal | 21.5 ± 2.1 | | | | 1.5 (0.44–5.75) | 0.472 |
| Recurrence | | | | | | |
| Negative | 17.6 ± 0.8 | 0.284 | 0.397 | 0.342 | 11.1 (2.88–42.5) | <0.001 |
| Positive | 15.3 ± 1.8 | | | | | |
| GAS5 fold | | | | | | |
| Under-expressed | 17.5 ± 0.9 | 0.765 | 0.581 | 0.642 | 0.96 (0.49–1.85) | 0.904 |
| Over-expressed | 16.9 ± 1.6 | | | | | |
| miR-34a fold | | | | | | |
| Under-expressed | 17.7 ± 0.9 | 0.460 | 0.453 | 0.415 | 1.14 (0.79–1.65) | 0.471 |
| Over-expressed | 16.1 ± 1.5 | | | | | |

Survival time is shown as mean and standard error, OS overall survival, HR (95% CI) Hazard ratio (95% confidence interval). Statistically significant values ($p < 0.05$) are shown in bold.

<https://doi.org/10.1371/journal.pone.0198231.t006>

and miR-9 which inhibits lncRNA MALAT1 [71]. Third, miRNAs and lncRNAs can both compete for the same binding site on mRNAs, an example of which is miR-485-5p and lncRNA BACE1AS competing for BACE1 mRNA [72]. Fourth and finally, another form of relationship exists between the two types; where the lncRNA (>200 nucleotide) is capable of generating smaller (<22 nucleotide) miRNAs such as the lncRNA H19 generating miR-675 [73]. GAS5 provides a perfect example for such interactions. For instance, GAS5 acts as a molecular sponge for many different microRNAs, including miR-21, miR-222, miR-196a, miR-205, miR-221 and miR-103. [16, 26, 74–77], all of which are related to cancer. Then again, both miR-21 and miR-222 can negatively regulate GAS5 [27, 78]. Also, three of the snoRNAs produced by GAS5 (U44, U74 and U78) can give rise to miRNAs [79], making GAS5 one of the lncRNAs generating miRNAs.

While functional validation has yet been required to prove the direct interaction between GAS5 and miR-34a, it is highly plausible. This is due to the already verified interaction between miR-34a and GAS1 (Growth arrest specific 1), another member of the GAS genes [42]. GAS1 is a protein coding gene that, similar to GAS5, exerts its tumor suppressor actions through arresting the cell cycle and stimulating apoptosis [80]. Ma et al. measured the expression of miR-34a and the GAS1 protein in papillary thyroid carcinoma; GAS1 was under-expressed, while miR-34a was over-expressed. Further analysis revealed that miR-34a binds to the 3'UTR of GAS1 causing its silencing, which in turn activates the RET oncogene [42]. Through the BLAST tool, we detected sequence homology between the GAS1 and the GAS5 genes, further raising the possibility of interaction of miRNA-34a with GAS5. Given that GAS5 is down-regulated and miR-34a is up-regulated in our study, tumorigenesis may be in such a case due to sponging of miR-34a by GAS5, where under-expression of GAS5 in the rapidly

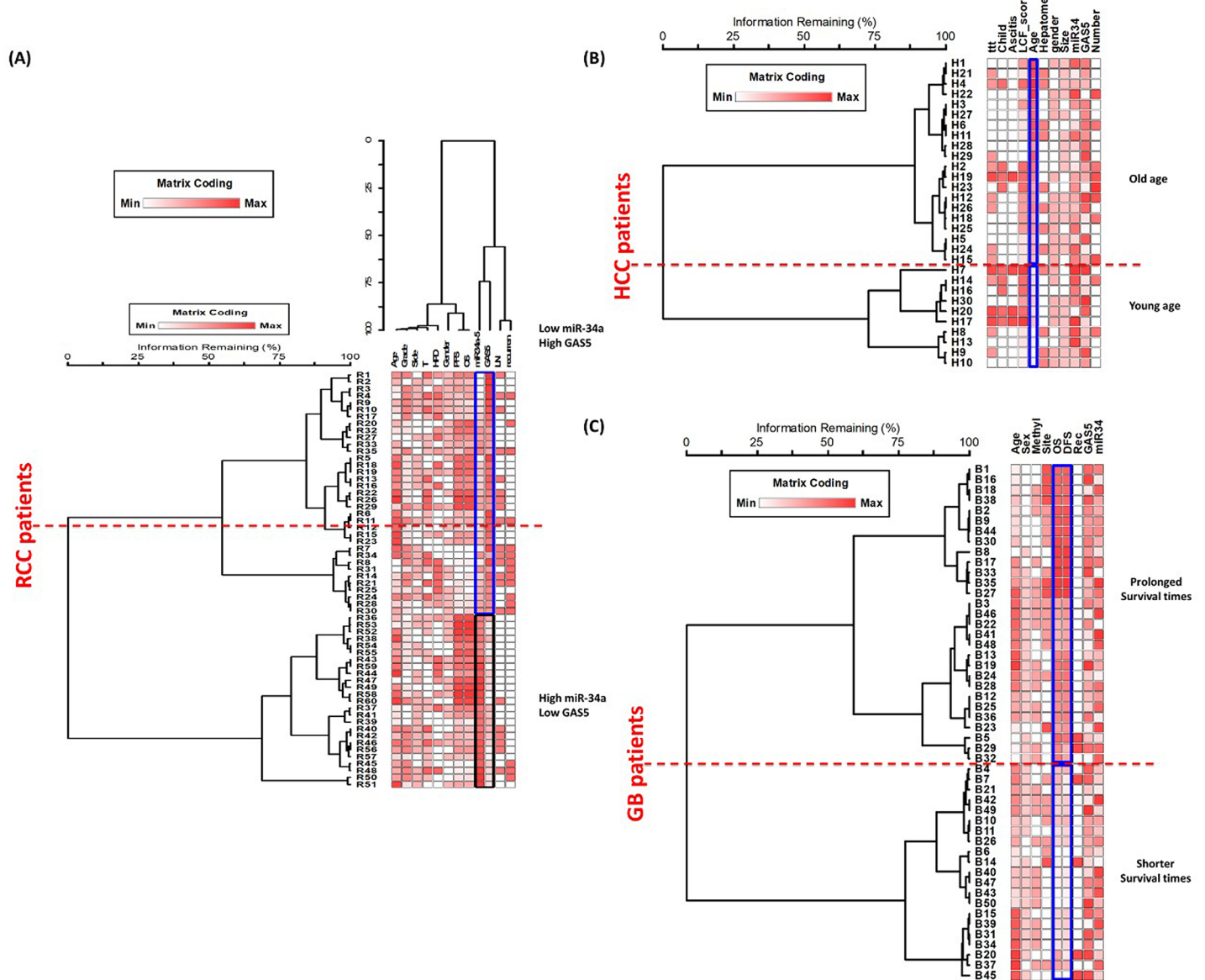


Fig 5. Multivariate analysis of patients according to combined transcriptomic signature of genes and clinicopathological features. (A) RCC, (B) GB, (C) HCC. RCC patients were divided based on GAS5 and miR-34a levels, GB patients were divided by survival times and HCC patients by age.

<https://doi.org/10.1371/journal.pone.0198231.g005>

dividing cancer cells causes release of the inhibition of miR-34a on its tumor suppressor targets, allowing for further tumor progression. Oppositely, the inverse correlation between the two could also suggest that miR-34a inhibits GAS5, making its under-expression a cause of cancer rather than a result, as in the case of the miR-34a-GAS1 interaction.

In patients with GB, both GAS5 and miR-34a levels were significantly down-regulated. Zhang et al. correlated the expression of five lncRNAs including GAS5 with GB and found that higher levels of GAS5 were associated with prolonged survival [81]. Zhao et al. found that GAS5 was under-expressed in glioma cell lines U87 and U251 and that its tumor suppressor role was through targeting miR-222 [16]. The same author, in a more recent study, added another miRNA to the targets of GAS5; miR-196a-5p, where GAS5 under-expression in human glioma stem cells enhanced tumor progression through inhibiting this miRNA [82].

Regarding the more controversial *miR-34a*, studies on brain cancer, including GB and glioma agree on its role as a tumor suppressor in this particular tissue; reviewed in [83], which fits in with its expression status in the present study.

MiR-34a expression levels in our study were not significant in the case of patients with HCC. *GAS5* levels, however, were under-expressed in HCC patients. In addition, lower *GAS5* levels were marginally associated with more numerous tumor foci. The same conclusions were reached by studies conducted by Tu et al., Chang et al. and Hu et al. who found that *GAS5* was under-expressed in HCC patients and predicted poor survival in those patients [15, 26, 84]. The latter study by Hu et al. found that under-expression of *GAS5* in HCC cell lines releases its sponging effect on oncomiR-21, which normally targets the two tumor suppressor genes *PDCD4* and *PTEN* [26]. On the contrary, according to Tao et al., *GAS5* was a proto-oncogene in HCC where they found an indel polymorphism in the promotor of *GAS5* that increased the risk of HCC in Chinese. *In vitro* analysis showed that the deletion allele of the polymorphism altered methylation of the *GAS5* promoter and was associated with higher levels of *GAS5* in HCC cell lines Sk-hep-1, Bel-7404 and Huh7. Further analysis provided evidence that the resulting over-expression of *GAS5* had an anti-apoptotic effect in those cell lines [85]. This divergence observed by Tao et al. could be due to racial differences. In other words, the allele causing *GAS5* over-expression might be more common in their studied population. To further confirm this probability, we searched the 1000 genome project phase 3 databases [86] for this indel polymorphism (position 1:173868254–173868258 (AGGCA/-)). We found that the frequency of the deletion allele was very high in Asians and Chinese in particular (28–40%) as compared to other races (3–12%), showing that in other populations the effect of the polymorphism on HCC and *GAS5* expression could be negligible.

Conclusions

In this study, we show that *GAS5* is under-expressed in three types of tumors, in addition to being associated with tumor prognosis in some types. Consequently, we believe that *GAS5* could potentially be used as a prognostic marker for cancer. Furthermore, we suppose that miR-34a might be a potential target of *GAS5*, or *vice versa*. However, further studies are required to validate this interaction.

Supporting information

S1 Table. *GAS5* alternative splicing transcripts.

(PDF)

S2 Table. *GAS5* common variants.

(PDF)

S3 Table. LncRNA *GAS5*-microRNA interaction.

(PDF)

S4 Table. Complementarity between *GAS5* transcripts and miR-34a-5p.

(PDF)

S5 Table. hsa-miR-34a pathways.

(PDF)

S1 Fig. Receiver Operating Characteristics (ROC) analysis for the prognostic value of the markers. RCC renal cell carcinoma, GB glioblastoma, HCC hepatocellular carcinoma, AUC area under curve, CTP Child-Turcotte-Pugh classification for liver cell failure. (TIF)

Acknowledgments

The authors thank the Center of Excellence in Molecular and Cellular Medicine and the Oncology Diagnostic Unit, Suez Canal University, Ismailia, Egypt for providing the facilities for performing the research work.

Author Contributions

Conceptualization: Eman A. Toraih, Mohammad H. Hussein, Manal S. Fawzy.

Data curation: Eman A. Toraih, Aya El-Wazir.

Formal analysis: Eman A. Toraih, Saleh Ali Alghamdi, Aya El-Wazir, Marwa M. Hosny, Mohammad H. Hussein.

Investigation: Eman A. Toraih, Manal S. Fawzy.

Methodology: Eman A. Toraih, Saleh Ali Alghamdi, Aya El-Wazir, Marwa M. Hosny, Moataz S. Khashana, Manal S. Fawzy.

Resources: Eman A. Toraih, Saleh Ali Alghamdi, Marwa M. Hosny, Mohammad H. Hussein, Moataz S. Khashana.

Supervision: Manal S. Fawzy.

Visualization: Aya El-Wazir.

Writing – original draft: Aya El-Wazir.

Writing – review & editing: Saleh Ali Alghamdi, Manal S. Fawzy.

References

1. WHO | Cancer [WWW Document], World Health Organization. Available from URL <http://www.who.int/mediacentre/factsheets/fs297/en/> (accessed 9.2.18).
2. Grandér D. How do mutated oncogenes and tumor suppressor genes cause cancer? *Med Oncol*. 1998; 15:20–6. <https://doi.org/10.1007/BF02787340> PMID: 9643526
3. ENCODE Project Consortium. An integrated encyclopedia of DNA elements in the human genome. *Nature*. 2012; 489:57–74. <https://doi.org/10.1038/nature11247> PMID: 22955616
4. Paraskevopoulou MD, Hatzigeorgiou AG. Analyzing MiRNA–LncRNA Interactions, in: Long Non-Coding RNAs, *Methods in Molecular Biology*. Humana Press, New York, NY, 2016; pp. 271–286. https://doi.org/10.1007/978-1-4939-3378-5_21
5. Bartonicek N, Maag JLV, Dinger ME. Long noncoding RNAs in cancer: mechanisms of action and technological advancements. *Mol Cancer*. 2016; 15:43. <https://doi.org/10.1186/s12943-016-0530-6> PMID: 27233618
6. Leva GD, Garofalo M, Croce CM. MicroRNAs in Cancer. *Annu Rev Pathol Mech Dis*. 2014; 9:287–314. <https://doi.org/10.1146/annurev-pathol-012513-104715>
7. Mannoor K, Liao J, Jiang F. Small nucleolar RNAs in cancer. *Biochim Biophys Acta*. 2012; 1826(1):121–128. <https://doi.org/10.1016/j.bbcan.2012.03.005> PMID: 22498252
8. Ng KW, Anderson C, Marshall EA, Minatel BC, Enfield KSS, Saprunoff HL, et al. Piwi-interacting RNAs in cancer: emerging functions and clinical utility. *Mol Cancer*. 2016; 15:5. <https://doi.org/10.1186/s12943-016-0491-9> PMID: 26768585
9. Lo P-K, Wolfson B, Zhou X, Duru N, Gernapudi R, Zhou Q. Noncoding RNAs in breast cancer. *Brief Funct Genomics*. 2016; 15:200–221. <https://doi.org/10.1093/bfpg/vel055> PMID: 26685283
10. Raho G, Barone V, Rossi D, Philipson L, Sorrentino V. The gas 5 gene shows four alternative splicing patterns without coding for a protein. *Gene*. 2000; 256:13–17. [https://doi.org/10.1016/S0378-1119\(00\)00363-2](https://doi.org/10.1016/S0378-1119(00)00363-2) PMID: 11054530

11. Smith CM, Steitz JA. Classification of gas5 as a Multi-Small-Nucleolar-RNA (snoRNA) Host Gene and a Member of the 5'-Terminal Oligopyrimidine Gene Family Reveals Common Features of snoRNA Host Genes. *Mol Cell Biol.* 1998; 18:6897–6909. PMID: [9819378](#)
12. Maden BE, Hughes JM. Eukaryotic ribosomal RNA: the recent excitement in the nucleotide modification problem. *Chromosoma.* 1997; 105:391–400. PMID: [9211966](#)
13. Schneider C, King RM, Philipson L. Genes specifically expressed at growth arrest of mammalian cells. *Cell.* 1988; 54:787–793. PMID: [3409319](#)
14. Coccia EM, Cicala C, Charlesworth A, Ciccarelli C, Rossi G B, Philipson L, et al. Regulation and expression of a growth arrest-specific gene (gas5) during growth, differentiation, and development. *Mol Cell Biol.* 1992; 12:3514–3521. PMID: [1630459](#)
15. Chang L, Li C, Lan T, Long Wu, Yufeng Yuan, Quanyan Luet, et al. Decreased expression of long non-coding RNA GAS5 indicates a poor prognosis and promotes cell proliferation and invasion in hepatocellular carcinoma by regulating vimentin. *Mol Med Rep.* 2016; 13:1541–1550. <https://doi.org/10.3892/mmr.2015.4716> PMID: [26707238](#)
16. Zhao X, Wang P, Liu J, Zheng J, Liu Y, Chen J, et al. Gas5 Exerts Tumor-suppressive Functions in Human Glioma Cells by Targeting miR-222. *Mol Ther.* 2015; 23:1899–1911. <https://doi.org/10.1038/mt.2015.170> PMID: [26370254](#)
17. Liang W, Lv T, Shi X, Liu H, Zhu Q, Zeng J, et al. Circulating long noncoding RNA GAS5 is a novel biomarker for the diagnosis of nonsmall cell lung cancer. *Medicine (Baltimore).* 2016; 95:e4608. <https://doi.org/10.1097/MD.0000000000004608>
18. Cao Q, Wang N, Qi J, Gu Z, Shen H. Long non-coding RNA-GAS5 acts as a tumor suppressor in bladder transitional cell carcinoma via regulation of chemokine (C-C motif) ligand 1 expression. *Mol Med Rep.* 2016; 13:27–34. <https://doi.org/10.3892/mmr.2015.4503> PMID: [26548923](#)
19. Yacqub-Usman K, Pickard MR, Williams GT. Reciprocal regulation of GAS5 lncRNA levels and mTOR inhibitor action in prostate cancer cells. *The Prostate* 2015; 75:693–705. <https://doi.org/10.1002/pros.22952> PMID: [25650269](#)
20. Pickard MR, Williams GT. Regulation of apoptosis by long non-coding RNA GAS5 in breast cancer cells: implications for chemotherapy. *Breast Cancer Res Treat.* 2014; 145:359–3570. <https://doi.org/10.1007/s10549-014-2974-y> PMID: [24789445](#)
21. Guo C, Song W-Q, Sun P, Jin L, Dai H-Y. LncRNA-GAS5 induces PTEN expression through inhibiting miR-103 in endometrial cancer cells. *J. Biomed. Sci.* 2015; 22:100. <https://doi.org/10.1186/s12929-015-0213-4> PMID: [26511107](#)
22. Lu X, Fang Y, Wang Z, Xie J, Zhan Q, Deng X, et al. Downregulation of gas5 increases pancreatic cancer cell proliferation by regulating CDK6. *Cell Tissue Res.* 2013; 354:891–896. <https://doi.org/10.1007/s00441-013-1711-x> PMID: [24026436](#)
23. Yin D, He X, Zhang E, Kong R, De W, Zhang Z. Long noncoding RNA GAS5 affects cell proliferation and predicts a poor prognosis in patients with colorectal cancer. *Med Oncol Northwood Lond Engl.* 2014; 31:253. <https://doi.org/10.1007/s12032-014-0253-8>
24. Qiao H-P, Gao W-S, Huo J-X, Yang Z-S. Long Non-coding RNA GAS5 Functions as a Tumor Suppressor in Renal Cell Carcinoma. *Asian Pac J Cancer Prev.* 2013; 14:1077–1082. <https://doi.org/10.7314/APJCP.2013.14.2.1077> PMID: [23621190](#)
25. Nakamura Y, Takahashi N, Kakegawa E, Yoshida K, Ito Y, Kayano H, et al. The GAS5 (growth arrest-specific transcript 5) gene fuses to BCL6 as a result of t(1;3) (q25;q27) in a patient with B-cell lymphoma. *Cancer Genet. Cytogenet.* 2008; 182:144–149. <https://doi.org/10.1016/j.cancergencyto.2008.01.013> PMID: [18406879](#)
26. Hu L, Ye H, Huang G, Luo F, Liu Y, Liu Y, et al. Long noncoding RNA GAS5 suppresses the migration and invasion of hepatocellular carcinoma cells via miR-21. *Tumour Biol.* 2016; 37:2691–2702. <https://doi.org/10.1007/s13277-015-4111-x> PMID: [26404135](#)
27. Zhang Z, Zhu Z, Watabe K, Zhang X, Bai C, Xu M, et al. Negative regulation of lncRNA GAS5 by miR-21. *Cell Death Differ.* 2013; 20:1558–1568. <https://doi.org/10.1038/cdd.2013.110> PMID: [23933812](#)
28. He L, He X, Lim LP, de Stanchina E, Xuan Z, Liang Y, et al. A microRNA component of the p53 tumour suppressor network. *Nature.* 2007; 447:1130–1134. <https://doi.org/10.1038/nature05939> PMID: [17554337](#)
29. Lodygin D, Tarasov V, Epanchintsev A, Berking C, Knyazeva T, Körner H, et al. Inactivation of miR-34a by aberrant CpG methylation in multiple types of cancer. *Cell Cycle.* 2008; 7:2591–2600. <https://doi.org/10.4161/cc.7.16.6533> PMID: [18719384](#)
30. Welch C, Chen Y, Stallings RL. MicroRNA-34a functions as a potential tumor suppressor by inducing apoptosis in neuroblastoma cells. *Oncogene.* 2007; 26:5017–5022. <https://doi.org/10.1038/sj.onc.1210293> PMID: [17297439](#)

31. Chim CS, Wong KY, Qi Y, Loong F, Lam WL, Wong LG, et al. Epigenetic inactivation of the miR-34a in hematological malignancies. *Carcinogenesis*. 2010; 31:745–750. <https://doi.org/10.1093/carcin/bgq033> PMID: 20118199
32. Ji Q, Hao X, Zhang M, Tang W, Yang M, Li L, et al. MicroRNA miR-34 inhibits human pancreatic cancer tumor-initiating cells. *PLoS One*. 2009; 4:e6816. <https://doi.org/10.1371/journal.pone.0006816> PMID: 19714243
33. Li N, Fu H, Tie Y, Hu Z, Kong W, Wu Y, et al. miR-34a inhibits migration and invasion by down-regulation of c-Met expression in human hepatocellular carcinoma cells. *Cancer Lett*. 2009; 275:44–53. <https://doi.org/10.1016/j.canlet.2008.09.035> PMID: 19006648
34. Shehata RH, Abdelmoneim SS, Osman OA, Hasanain AF, Osama A, Abdelmoneim SS, et al. Deregulation of miR-34a and Its Chaperon Hsp70 in Hepatitis C virus-Induced Liver Cirrhosis and Hepatocellular Carcinoma Patients. *Asian Pacific Journal of Cancer Prevention. APJCP*. 2017; 18(9):2395–2401. <https://doi.org/10.22034/APJCP.2017.18.9.2395> PMID: 28950684
35. Li Y, Guessous F, Zhang Y, Dipierro C, Kefas B, Johnson E, et al. MicroRNA-34a inhibits glioblastoma growth by targeting multiple oncogenes. *Cancer Res*. 2009; 69:7569–76. <https://doi.org/10.1158/0008-5472.CAN-09-0529> PMID: 19773441
36. Toraih EA, Aly NM, Abdallah HY, Al-Qahtani SA, Shaalan AA, Hussein MH, et al. MicroRNA-target cross-talks: Key players in glioblastoma multiforme. *Tumour Biol*. 2017; 39(11):1010428317726842. <https://doi.org/10.1177/1010428317726842>
37. Kato M1, Paranjape T, Müller RU, Nallur S, Gillespie E, Keane K, et al. The mir-34 microRNA is required for the DNA damage response in vivo in *C. elegans* and in vitro in human breast cancer cells. *Oncogene*. 2009; 28:2419–2424. <https://doi.org/10.1038/onc.2009.106> PMID: 19421141
38. Wiggins JF, Ruffino L, Kelnar K, Omotola M, Patrawala L, Brown D, et al. Development of a lung cancer therapeutic based on the tumor suppressor microRNA-34. *Cancer Res*. 2010; 70:5923–5930. <https://doi.org/10.1158/0008-5472.CAN-10-0655> PMID: 20570894
39. Tazawa H, Tsuchiya N, Izumiya M, Nakagama H. Tumor-suppressive miR-34a induces senescence-like growth arrest through modulation of the E2F pathway in human colon cancer cells. *Proc Natl Acad Sci USA*. 2007; 104:15472–15477. <https://doi.org/10.1073/pnas.0707351104> PMID: 17875987
40. Liu H, Brannon AR, Reddy AR, Alexe G, Seiler MW, Arreola A, et al. Identifying mRNA targets of microRNA dysregulated in cancer: with application to clear cell Renal Cell Carcinoma. *BMC Syst Biol*. 2010; 4:51. <https://doi.org/10.1186/1752-0509-4-51> PMID: 20420713
41. Toraih EA, Ibrahim AT, Fawzy MS, Hussein MH, Al-Qahtani SAM, Shaalan AAM. MicroRNA-34a: A Key Regulator in the Hallmarks of Renal Cell Carcinoma. *Oxid Med Cell Longev*. 2017; 2017:3269379. <https://doi.org/10.1155/2017/3269379> PMID: 29104726
42. Ma Y, Qin H, Cui Y. MiR-34a targets GAS1 to promote cell proliferation and inhibit apoptosis in papillary thyroid carcinoma via PI3K/Akt/Bad pathway. *Biochem Biophys Res Commun*. 2013; 441:958–963. <https://doi.org/10.1016/j.bbrc.2013.11.010> PMID: 24220341
43. Marsh EE, Lin Z, Yin P, Milad M, Chakravarti D, Bulun SE. Differential expression of microRNA species in human uterine leiomyoma versus normal myometrium. *Fertil Steril*. 2008; 89:1771–1776. <https://doi.org/10.1016/j.fertnstert.2007.05.074> PMID: 17765232
44. Llovet JM, Fuster J, Bruix J. Barcelona-Clinic Liver Cancer Group. The Barcelona approach: diagnosis, staging, and treatment of hepatocellular carcinoma. *Liver Transpl*. 2004; 10:S115–120. <https://doi.org/10.1002/lt.20034> PMID: 14762851
45. Toraih EA, Fawzy MS, El-Falouji AI, Hamed EO, Nemr NA, Hussein MH, et al. Stemness-Related Transcriptional Factors and Homing Gene Expression Profiles in Hepatic Differentiation and Cancer. *Mol Med*. 2016; 22:653–663. <https://doi.org/10.2119/molmed.2016.00096> PMID: 27623812
46. Toraih EA, Fawzy MS, Mohammed EA, Hussein MH, El-Labban MM. MicroRNA-196a2 Biomarker and Targetome Network Analysis in Solid Tumors. *Mol Diagn Ther*. 2016; 20:559–577. <https://doi.org/10.1007/s40291-016-0223-2> PMID: 27342110
47. Bustin SA, Benes V, Garson JA, Hellemans J, Huggett J, Kubista M, et al. The MIQE guidelines: minimum information for publication of quantitative real-time PCR experiments. *Clin Chem*. 2009; 55:611–622. <https://doi.org/10.1373/clinchem.2008.112797> PMID: 19246619
48. Toraih EA, Mohammed EA, Farrag S, Ramsis N, Hosny S. Pilot Study of Serum MicroRNA-21 as a Diagnostic and Prognostic Biomarker in Egyptian Breast Cancer Patients. *Mol Diagn Ther*. 2015; 19:179–190. <https://doi.org/10.1007/s40291-015-0143-6> PMID: 26063582
49. Valente V, Teixeira SA, Neder L, Okamoto OK, Oba-Shinjo SM, Marie SK, et al. Selection of suitable housekeeping genes for expression analysis in glioblastoma using quantitative RT-PCR. *Ann Neurosci*. 2014; 21(2):62–63. <https://doi.org/10.5214/ans.0972.7531.210207> PMID: 25206063

50. Aithal MGS, Rajeswari N. Validation of Housekeeping Genes for Gene Expression Analysis in Glioblastoma Using Quantitative Real-Time Polymerase Chain Reaction. *Brain Tumor Res Treat.* 2015; 3:24–29. <https://doi.org/10.14791/btrt.2015.3.1.24> PMID: 25977903
51. Livak KJ, Schmittgen TD. Analysis of relative gene expression data using real-time quantitative PCR and the 2⁻(-Delta Delta C (T)) Method. *Methods.* 2001; 25:402–408. <https://doi.org/10.1006/meth.2001.1262> PMID: 11846609
52. McCune B, Mefford MJ. PC-ORD. Multivariate Analysis of Ecological Data. Version 6. MjM Software, Gleneden Beach, Oregon, USA, 2011.
53. Yamashita R, Suzuki Y, Takeuchi N, Wakaguri H, Ueda T, Sugano S, et al. Comprehensive detection of human terminal oligo-pyrimidine (TOP) genes and analysis of their characteristics. *Nucleic Acids Res.* 2008; 36:3707–3715. <https://doi.org/10.1093/nar/gkn248> PMID: 18480124
54. Cheng T, Wang L, Li Y, Huang C, Zeng L, Yang J. Differential microRNA expression in renal cell carcinoma. *Oncol Lett.* 2013; 6:769–776. <https://doi.org/10.3892/ol.2013.1460> PMID: 24137408
55. Munari E, Marchionni L, Chitre A, Hayashi M, Martignoni G, Brunelli M, et al. Clear cell papillary renal cell carcinoma: micro-RNA expression profiling and comparison with clear cell renal cell carcinoma and papillary renal cell carcinoma. *Hum Pathol.* 2014; 45:1130–1138. <https://doi.org/10.1016/j.humpath.2014.01.013> PMID: 24703100
56. Fritz HK, Gustafsson A, Ljungberg B, Ceder Y, Axelson H, Dahlbäck B. The Axl-Regulating Tumor Suppressor miR-34a Is Increased in ccRCC but Does Not Correlate with Axl mRNA or Axl Protein Levels. *PLoS One.* 2015; 10:e0135991. <https://doi.org/10.1371/journal.pone.0135991> PMID: 26287733
57. Bhatt K, Zhou L, Mi QS, Huang S, She JX, Dong Z. MicroRNA-34a is induced via p53 during cisplatin nephrotoxicity and contributes to cell survival. *Mol Med.* 2010; 16:409–416. <https://doi.org/10.2119/molmed.2010.00002> PMID: 20386864
58. Yadav S, Khandelwal M, Seth A, Saini AK, Dogra PN, Sharma A. Serum microRNA Expression Profiling: Potential Diagnostic Implications of a Panel of Serum microRNAs for Clear Cell Renal Cell Cancer. *Urology.* 2017; 104:64–69. <https://doi.org/10.1016/j.urology.2017.03.013> PMID: 28336290
59. Zhang EB, Kong R, Yin DD, You LH, Sun M, Han L, et al. Long noncoding RNA ANRIL indicates a poor prognosis of gastric cancer and promotes tumor growth by epigenetically silencing of miR-99a/miR-449a. *Oncotarget.* 2014; 5:2276–2292. <https://doi.org/10.18632/oncotarget.1902> PMID: 24810364
60. Weng W, Wang M, Xie S, Long Y, Li F, Sun F, et al. YY1-C/EBP α -miR34a regulatory circuitry is involved in renal cell carcinoma progression. *Oncol Rep.* 2014; 31:1921–1927. <https://doi.org/10.3892/or.2014.3005> PMID: 24481728
61. Yu G, Li H, Wang J, Gumireddy K, Li A, Yao W, et al. miRNA-34a Suppresses Cell Proliferation and Metastasis by Targeting CD44 in Human Renal Carcinoma Cells. *J Urol.* 2014; 192:1229–1237. <https://doi.org/10.1016/j.juro.2014.05.094> PMID: 24866595
62. Yamamura S, Saini S, Majid S, Hirata H, Ueno K, Chang I, et al. MicroRNA-34a suppresses malignant transformation by targeting c-Myc transcriptional complexes in human renal cell carcinoma. *Carcinogenesis.* 2012; 33:294–300. <https://doi.org/10.1093/carcin/bgr286> PMID: 22159222
63. Liu F, Chen N, Gong Y, Xiao R, Wang W, Pan Z. The long non-coding RNA NEAT1 enhances epithelial-to-mesenchymal transition and chemoresistance via the miR-34a/c-Met axis in renal cell carcinoma. *Oncotarget.* 2017; 8:62927–62938. <https://doi.org/10.18632/oncotarget.17757> PMID: 28968960
64. Bai XY, Ma Y, Ding R, Fu B, Shi S, Chen XM. miR-335 and miR-34a Promote Renal Senescence by Suppressing Mitochondrial Antioxidative Enzymes. *J Am Soc Nephrol.* 2011; 22:1252–1261. <https://doi.org/10.1681/ASN.2010040367> PMID: 21719785
65. Collado M, Blasco MA, Serrano M. Cellular Senescence in Cancer and Aging. *Cell.* 2007; 130:223–233. <https://doi.org/10.1016/j.cell.2007.07.003> PMID: 17662938
66. Zhou Y, Xiong M, Niu J, Sun Q, Su W, Zen K, et al. Secreted fibroblast-derived miR-34a induces tubular cell apoptosis in fibrotic kidney. *J Cell Sci.* 2014; 127:4494–4506. <https://doi.org/10.1242/jcs.155523> PMID: 25107369
67. Borrell B. How accurate are cancer cell lines? *Nature.* 2010; 463:858. <https://doi.org/10.1038/463858a> PMID: 20164888
68. Clark MJ, Homer N, O'Connor BD, Chen Z, Eskin A, Lee H, et al. U87MG Decoded: The Genomic Sequence of a Cytogenetically Aberrant Human Cancer Cell Line. *PLoS Genet.* 2010; 6:e1000832. <https://doi.org/10.1371/journal.pgen.1000832> PMID: 20126413
69. Yoon JH, Abdelmohsen K, Srikantan S, Yang X, Martindale JL, De S, et al. LincRNA-p21 suppresses target mRNA translation. *Mol Cell.* 2012; 47:648–655. <https://doi.org/10.1016/j.molcel.2012.06.027> PMID: 22841487

70. Wang Y, Xu Z, Jiang J, Xu C, Kang J, Xiao L, et al. Endogenous miRNA Sponge lincRNA-RoR Regulates Oct4, Nanog, and Sox2 in Human Embryonic Stem Cell Self-Renewal. *Dev Cell*. 2013; 25:69–80. <https://doi.org/10.1016/j.devcel.2013.03.002> PMID: 23541921
71. Leucci E, Patella F, Waage J, Holmström K, Lindow M, Porse B, et al. microRNA-9 targets the long non-coding RNA MALAT1 for degradation in the nucleus. *Sci Rep*. 2013; 3:2535. <https://doi.org/10.1038/srep02535> PMID: 23985560
72. Faghihi MA, Zhang M, Huang J, Modarresi F, Van der Brug MP, Nalls MA, et al. Evidence for natural antisense transcript-mediated inhibition of microRNA function. *Genome Biol*. 2010; 11:R56. <https://doi.org/10.1186/gb-2010-11-5-r56> PMID: 20507594
73. Keniry A, Oxley D, Monnier P, Kyba M, Dandolo L, Smits G, et al. The H19 lincRNA is a developmental reservoir of miR-675 that suppresses growth and Igf1r. *Nat Cell Biol*. 2012; 14:659–665. <https://doi.org/10.1038/ncb2521> PMID: 22684254
74. Guo C, Song WQ, Sun P, Jin L, Dai HY. LncRNA-GAS5 induces PTEN expression through inhibiting miR-103 in endometrial cancer cells. *J Biomed Sci*. 2015; 22:100. <https://doi.org/10.1186/s12929-015-0213-4> PMID: 26511107
75. Xue D, Zhou C, Lu H, Xu R, Xu X, He X. LncRNA GAS5 inhibits proliferation and progression of prostate cancer by targeting miR-103 through AKT/mTOR signaling pathway. *Tumor Biol*. 2016; 37:16187–16197. <https://doi.org/10.1007/s13277-016-5429-8>
76. Yang W, Hong L, Xu X, Wang Q, Huang J, Jiang L. LncRNA GAS5 suppresses the tumorigenesis of cervical cancer by downregulating miR-196a and miR-205. *Tumour Biol*. 2017; 39:1010428317711315. <https://doi.org/10.1177/1010428317711315> PMID: 28671039
77. Ye K, Wang S, Zhang H, Han H, Ma B, Nan W. Long Noncoding RNA GAS5 Suppresses Cell Growth and Epithelial-Mesenchymal Transition in Osteosarcoma by Regulating the miR-221/ARHI Pathway. *J Cell Biochem*. 2017; 118:4772–4781. <https://doi.org/10.1002/jcb.26145> PMID: 28519068
78. Yu F, Zheng J, Mao Y, Dong P, Lu Z, Li G, et al. Long Non-coding RNA Growth Arrest-specific Transcript 5 (GAS5) Inhibits Liver Fibrogenesis through a Mechanism of Competing Endogenous RNA. *J Biol Chem*. 2015; 290:28286–28298. <https://doi.org/10.1074/jbc.M115.683813> PMID: 26446789
79. Brameier M, Herwig A, Reinhardt R, Walter L, Gruber J. Human box C/D snoRNAs with miRNA like functions: expanding the range of regulatory RNAs. *Nucleic Acids Res*. 2011; 39:675–686. <https://doi.org/10.1093/nar/gkq776> PMID: 20846955
80. Domínguez-Monzón G, Benítez JA, Vergara P, Lorenzana R, Segovia J. Gas1 inhibits cell proliferation and induces apoptosis of human primary gliomas in the absence of Shh. *Int J Dev Neurosci*. 2009; 27:305–313. <https://doi.org/10.1016/j.ijdevneu.2009.03.009> PMID: 19460624
81. Zhang XQ, Sun S, Lam KF, Kiang KM, Pu JK, Ho AS, et al. A long non-coding RNA signature in glioblastoma multiforme predicts survival. *Neurobiol Dis*. 2013; 58:123–131. <https://doi.org/10.1016/j.nbd.2013.05.011> PMID: 23726844
82. Zhao X, Liu Y, Zheng J, Liu X, Chen J, Liu L, et al. GAS5 suppresses malignancy of human glioma stem cells via a miR-196a-5p/FOXO1 feedback loop. *Biochim Biophys Acta*. 2017; 1864:1605–1617. <https://doi.org/10.1016/j.bbamcr.2017.06.020>
83. Møller HG, Rasmussen AP, Andersen HH, Johnsen KB, Henriksen M, Duroux M. A Systematic Review of MicroRNA in Glioblastoma Multiforme: Micro-modulators in the Mesenchymal Mode of Migration and Invasion. *Mol Neurobiol*. 2013; 47:131–144. <https://doi.org/10.1007/s12035-012-8349-7> PMID: 23054677
84. Tu ZQ, Li RJ, Mei JZ, Li XH. Down-regulation of long non-coding RNA GAS5 is associated with the prognosis of hepatocellular carcinoma. *Int. J Clin Exp Pathol*. 2014; 7:4303–4309. PMID: 25120813
85. Tao R, Hu S, Wang S, Zhou X, Zhang Q, Wang C, et al. Association between indel polymorphism in the promoter region of lincRNA GAS5 and the risk of hepatocellular carcinoma. *Carcinogenesis*. 2015; 36:1136–1143. <https://doi.org/10.1093/carcin/bgv099> PMID: 26163879
86. The 1000 Genomes Project Consortium. A global reference for human genetic variation. *Nature*. 2015; 526:68–74. <https://doi.org/10.1038/nature15393> PMID: 26432245